Achimer
http://archimer.ifremer.fr

Aerial surveys to monitor bluefin tuna abundance and track efficiency of management measures

Bauer Robert [1], Bonhommeau Sylvain [1], Brisset Blandine [1], Fromentin Jean-Marc [1, *]

[1] IFREMER, UMR Marbec, F-34203 Sete, France.

* Corresponding author : Jean-Marc Fromentin, email address : jean.marc.fromentin@ifremer.fr

Abstract :

Conservation and management measures for exploited fish species rely on our ability to monitor variations in population abundance. In the case of the eastern stock of Atlantic bluefin tuna (ABFT), recent changes in management policies have strongly affected the reliability of fishery-dependent indicators due to drastic changes in fishing season/area, fisheries selectivity and strategy. However, fishery-independent indices of abundance are rare for large pelagic fish, and obtaining them is often costly and labor intensive. Here, we show that scientific aerial surveys are an appropriate tool for monitoring juvenile bluefin tuna abundance in the Mediterranean. We present an abundance index based on 62 aerial surveys conducted since 2000, using 2 statistical approaches to deal with the sampling strategy: line and strip transects. Both approaches showed a significant increase in juvenile ABFT abundance in recent years, resulting from the recovery plan established in 2007. Nonetheless, the estimates from the line transect method appear to be more robust and stable. This study provides essential information for fisheries management. Expanding the spatial coverage to other nursery grounds would further increase the reliability and representativeness of this index.

Keywords : *Thunnus thynnus*, Index of abundance, Fishery-independent, Gulf of Lions, Mediterranean Sea, Strip transect, Distance sampling

Introduction

Declines in the Atlantic bluefin tuna *Thunnus thynnus* (ABFT) stocks, mostly resulting from extensive over-fishing, have been widely publicized in recent decades. The overexploitation of this species has been driven by both high fishing pressure and failure of management regulations (Fromentin *et al.* 2014). To counteract this trend, a multi-annual stock recovery plan was implemented in 2007 by the International Commission for the Conservation of Atlantic Tunas (ICCAT). This plan included significant restrictions of the fishing season and, later, on the quotas and minimum landing size as well as a significant reinforcement of the control of fishing activity (ICCAT 2006). These measures have had considerable impacts on the spatial patterns of tuna fleets and thus compromised the reliability of fisheries-derived abundance indices, in particular catch per unit effort (CPUE), used to monitor changes in the stock. Fisheries-independent information is thus essential to overcome this uncertainty. Tagging programs as well as larval and acoustic surveys can provide such information but are constrained by high costs and effort resulting from the broad scale at which they need to be implemented (Josse *et al.* 2000, Hobday *et al.* 2009, Fujioka *et al.* 2010, Ingram Jr *et al.* 2013, Leroy *et al.* 2015). These methods are also yet to be fully integrated

34 into the assessment models, particularly movement and stock composition. An alternative and more
35 effective source could be the use of aerial surveys to obtain tuna school counts (Polacheck *et al.* 1998). In
36 fact, spotter aircrafts have been used for a long time in purse seine fisheries to assist in locating tuna
37 schools (e.g. since 1974 in the Mediterranean; Petit *et al.* 1990), and their efficiency has previously been
38 demonstrated (Scott and Flittner 1972).
39 The use of aerial surveys for estimating animal densities has a long tradition in wildlife research and
40 management (Buckland *et al.* 2001), and such surveys are increasingly applied to marine organisms (e.g.
41 sea turtles and marine mammals; Lauriano *et al.* 2011, Panigada *et al.* 2011, de Oliveira Alves *et al.* 2013).
42 There is a growing interest in the potential use of aerial surveys for tuna stock assessment (Hoggard
43 1995, Polacheck *et al.* 1998, Lutcavage and Newlands 1999, Di Natale 2011). Promising results have been
44 obtained from aerial surveys on juvenile Southern bluefin tuna *Thunnus maccoyii* (age 2−4, 8−30 kg) in
45 the Great Australian Bight that are now used to construct an index of abundance (Eveson *et al.* 2012).
46 In the case of ABFT, aerial surveys on mature individuals (~196 cm, >226 kg) have been conducted in
47 the Gulf of Maine and along their migration pathways at the Great Bahama Banks, known as the "Tuna
48 Alley" (Hoggard 1995, Lutcavage and Kraus 1997, Lutcavage and Newlands 1999, Newlands *et al.* 2006).
49 However, the majority of these operations were performed using commercial spotter pilots and lacked a
50 rigorous statistical sampling design.
51 In this study, we illustrate the results from aerial surveys conducted since 2000 on juvenile ABFT (70−115
52 cm, < 30 kg, 2−4 yr) in the Gulf of Lions (GoL) (Bonhommeau *et al.* 2010, Fromentin *et al.* 2013). In
53 order to monitor population fluctuation, it is crucial to assess juvenile abundance, in particular to rapidly
54 assess the success of management measures or to identify effects caused by fisheries or environmental
55 changes. In this regard, nursery grounds represent essential survey areas. The GoL, with its large shelf
56 region and numerous canyons, represents one such area for ABFT (Farrugio *et al.* 1977). This region is
57 considered one of the most productive areas in the Mediterranean Sea, in contrast to the oligotrophic
58 conditions typically encountered throughout this basin. Based on this dataset, we present an abundance
59 index for juvenile ABFT in the Northwestern Mediterranean Sea. Two competing statistical methods
60 to derive density estimates from aerial surveys, the strip and line transect approaches—inconsistently
61 applied by the scientific community—are evaluated and the required methodological adaptations for
62 ABFT are discussed. Effects of recently implemented management measures on population trends are
63 investigated.

MATERIALS AND METHODS

Aerial surveys

66 Aerial surveys of juvenile Atlantic bluefin tuna were carried out in GoL over 2000 to 2003 and 2009
67 to present during August to October (Bonhommeau *et al.* 2010, Fromentin *et al.* 2013). This period
68 corresponded to the main fishing season in this area (Fromentin and Powers 2005). Young bluefin tuna
69 (here mostly ages 1 to 4) are easily detected by plane during feeding bouts when they swim or jump at
70 the surface (Fig. 1; Scott and Flittner 1972). Surveys were carried out at the same time of day (around
71 noon when the sun is at its highest, to avoid sun glare) and only under favorable weather conditions, i.e.
72 sunny sky and low wind speed (<28 km h^{-1}). Surveys took place aboard a Cessna C 337 "Push Pull"
73 from 2000 to 2011 and since 2012 aboard a Cessna 208 ISR, at 1000 and 1500 ft (305 and 457 m) above
74 the sea level, respectively.
75 Tuna schools were spotted by 1 to 3 trained scientific observers, from both sides of the plane/transects,
76 while the pilots provided supplementary sightings on the transect line. During each survey, a GPS
77 recorded the position of the plane every 30 s, while waypoints of sighted tuna schools were recorded
78 manually by the observers (we usually used 2 GPS devices, onboard GPS and a manual device, Garmin
79 GPS III PILOT). A standard survey consists of 10 vertical transects across the GoL region (Fig. 2),
80 with a total length of 1120 km (including off-route effort), spaced by an inter-transect distance of 13.8

km. At this distance, double counting of schools on subsequent transect lines due to tuna migrations is unlikely, because tunas are almost exclusively sighted feeding and not migrating (unlike in the Bahama banks, where ABFT are basically migrating at the surface). Furthermore, the use of the GPS allowed us to identify schools that had been already observed during the previous legs and thus avoid double counting if the school had remained roughly at the same place. All transect could be surveyed within 6 h at a constant speed of 200 km h^{-1} with the Cessna 208 ISR (the duration of each cruise can change according to the number of sightings). The maximum possible distance that could be covered by the first plane (the Cessna C 337) was limited due to fuel tank capacity and required that the route be split into 2 parts, a western and an eastern component, divided around 4.58° E. Both of these components were each surveyed within 4 h during different, usually subsequent, days. The aircraft change in 2012 allowed us also to georeference tuna schools directly from the transect line as well as to record the entire survey using a WESCAM MX-15HDi camera with built-in GPS. By contrast, during previous surveys, conducted on board the Cessna 337C, position records were taken while circling above spotted schools, which required the plane to leave and return to the transect line. Sightings generally included tuna schools of varying size feeding on small pelagic fish (e.g. anchovies or sardines) and which were regularly accompanied by sea birds and less often by whales, dolphins or other tuna species. Detected schools were hence classified by size, depending on the size of the produced surface disturbance (**"small"** for single to few individuals, **"medium"** for several individuals and **"large"** for a large area of surfacing and hunting tunas; Figs. 1 & S1). In some cases, schools occurred in short succession, very close to each other, so that only 1 waypoint was taken for several schools. Since 2009, we encountered areas with numerous tuna schools. School counting in these areas was particularly difficult due to the high number and the dynamics of the schools (which appeared/disappeared rapidly). To describe these sightings, we created a new category (**"aggregation zone",** Fig. 1). In addition to the position, number and size of tuna schools, the observers on board the aircraft and weather conditions (e.g. clouds, sea state) were recorded for each survey. Transect sections with heavy cloud cover or breaking waves were skipped and therefore discarded from subsequent analysis.

Data analysis

Data accuracy

GPS allowed us to obtain accurate positions of the route and sightings and thus reliable perpendicular distances, which are crucial for distance sampling theory (Buckland *et al.* 2001). The perpendicular distance is simply the shortest distance between the route and the spotted tuna school (Fig. 1). This distance is used as the input for subsequent analyses, the strip and line transect modeling (see below). Potential sources of errors in the calculation of perpendicular distances may include the precision at which transect routes are kept by the plane and the precision of school positions records. To reduce bias caused by systematic route deviations, perpendicular distances were calculated based on actual plane and not on intended flight routes tracks. For this purpose, sections with off-road trips, made until 2012 to take tuna school positions, were discarded and interpolated. Due to this sampling practice, the accuracy of related school positions was assessed. Since actual school positions were not available as reference points, it was assumed that the accuracy of position records may approximate the reaction time of observers, specifically, the distance traveled within this time. Assuming a reaction time of 1 or 2 s and an average plane speed of 56 m s^{-1} (200 km h^{-1}), the precision of position records made until 2012 could vary between 56 and 120 m. By contrast, position records obtained since 2012 on board of the Cessna 208 were of high accuracy because of the WESCAM MX-15HDi camera that calculated the GPS position of the targeted object. The overall sampling error made was therefore considered to be small, in particular with regard to the large distance range at which tuna schools can be detected (see below). Another, more common sampling practice in aerial surveys, where the positions of sighted objects are not directly measured, is to back-calculate perpendicular distances to sighted objects from sighting angles

128   and the aircraft altitude (Beavers and Ramsey 1998, Andriolo *et al.* 2006). Here, sighting angles are
129   measured by an inclinometer while the object of interest is abeam the aircraft. This requires additional
130   handling time by the observer, which makes this method less applicable for aerial surveys conducted at a
131   high traveling speed, where objects can pass through the detection range in a few seconds, partly in swift
132   succession. A comparison of the accuracy of both sampling methods is given by Marques *et al.* (2006).

Strip and line transect modeling

134   Two distinct approaches were applied to derive density and abundance estimates from the number
135   of sighted tuna schools, known as strip and line transect approaches (Buckland *et al.* 2001, Thomas
136   *et al.* 2012). Both methods rely on the sighting frequency of investigated objects, in particular their
137   perpendicular distance to the transect line. A related key assumption is that the detection probability is
138   certain on the transect line but decreasing with increasing distance. In the strip transect approach, the
139   (perpendicular) sighting distance frequency distribution (SDFD, Fig. 3) is truncated at a distance where
140   the detection probability is still certain and thus constant (Fig. 1). The object density is then derived by:

$$\hat{D}_i = \frac{n_i}{2wL},\tag{1}$$

141   where $\hat{D}_i$ is the density estimate (number per unit area) of survey *i*, and n_i is the number of objects (tuna
142   schools) detected during survey *i*, on a transect of length *L* and within a distance *w*. The line transect
143   approach aims to estimate the detection probability per distance (detectability *P*) and thus to calculate
144   the percentage of sighted and non-sighted objects. It thus follows an altered version of Eq. 1, that is:

$$\hat{D}_i = \frac{n_i}{2wLP}\tag{2}$$

145   The detectability *P*, also known as observability or sightability (Pierce *et al.* 2012), is estimated by
146   fitting a "**detection function**" to the SDFD (Fig. 3) and may depend on other variables (e.g. school size).
147   In theory, the shape of the SDFD and thus the detection function resembles that of a monotonically
148   decreasing, reverse-sigmoidal curve, showing a shoulder under which detection remains almost certain
149   and is unaffected by other variables (Buckland *et al.* 2001). Again, in strip transect theory, the data is
150   truncated to this shoulder area, and *w* corresponds to the shoulder width. Due to the rather spiked shape
151   of the SDFD, such a shoulder cannot be easily detected in the present dataset. Therefore, we selected
152   3 truncation levels (1.85, 2.8 and 3.7 km, corresponding to 1, 1.5 and 2 nm, Fig. 3) for which strip
153   transect densities were calculated and compared. Higher truncation was not considered to avoid data
154   omission and maintain the spatial representativeness. For line transects, data truncation is performed
155   to exclude outliers, in particular secondary sightings, and thus to facilitate modeling. According to
156   common practice, we discarded 5–10% of the largest distances, which correspond in the present study to
157   a band width of 4.5 and 3.5 km (Buckland *et al.* 1993). Line transect analyses were conducted using
158   the *ddf* - and *dht*- functions of the "mrds"-package (Laake *et al.* 2013) of the statistical language R
159   (R Core Team 2014). Two different key functions, the half normal and hazard rate, were applied in
160   the modeling of the detection probability. As mentioned above, the detectability of objects might be
161   affected by multiple factors. These factors can in turn affect the shape of the detection function and
162   may provide a more reasonable fit when included as covariates in line transect modeling, which is known
163   as multi-covariate distance sampling (MCDS; Marques and Buckland 2004, Thomas *et al.* 2012). For
164   instance, under higher sea state, more distant schools might be less detectable, causing a narrower shape
165   of the detection function. In the present study, the number and combination (team) of observers on
166   board as well as the sea state, the plane used and the school size were considered as possible covariates
167   affecting the detectability of tuna schools. As an indicator for the sea state, 0.25 degree, daily sea
168   surface wind speeds over the Mediterranean, derived from the NOAA Blended Sea Winds data set, were
169   used (`http://www.ncdc.noaa.gov/oa/rsad/air-sea/seawinds.html`). Daily average wind speeds in

the study area were calculated, and in case of surveys before 2012, the average of the respective sub-area, west or east of 46.5° E, were extracted. Absolute and Beaufort scale were also applied in the modeling for comparison.

Regarding the covariate school size, co-occurring schools with only 1 GPS record were treated as 1 sighted object for which the school size information was summarized. The treatment of the aggregation zones was more problematic, as only a few sighting positions referred to a large but "uncountable" amount of tuna schools in an area of a few nautical miles. Due to their rarity and the fact that they could not be summarized by a single GPS position, these sightings could not be introduced in the line transect modeling and treated as the other sightings. Because aggregation zones were large and much more easily detectable, it was assumed that they were always detected. As such, they were not modeled but were added directly to density estimates.

Line transect models were selected based on Akaike's information criterion (AIC) and further evaluated using goodness of fit tests (q-q plots, Cramer-von Mises and Kolmogorov-Smirnov tests).

Tuna densities in the GoL

For both modeling approaches, line and strip transects, school density estimates were derived for each school size class and each survey. In line transect modeling, this was achieved by running the "*dht*"-function on each survey and school size class separately. To obtain tuna density estimates in number of fish per surface area, the number of tunas per school is needed as a conversion factor. Since only jumping or near-surface individuals are seen by observers, the true number of tunas per school cannot be estimated from a plane. However, the total tuna number of tuna for the different school sizes might be reflected by the catch from purse seiners (PS) targeting free-swimming tuna schools in that area. To estimate school size, we therefore selected data of single PS sets from French PS that were operating in the GoL during the aerial survey season (August to October) in 2000–2007, assuming that a single PS set corresponds to a single school. A total number of 594 PS sets was finally retained. To identify different school size groups, a Gaussian mixture model was applied to the PS dataset, using the "*mixmodCluster*" function from the R-package "Rmixmod" (Auder *et al.* 2014). Four modes were detected in accordance to the 4 school size classes considered in this study (Fig. 4). Each mode is described by a normal distribution whose variance is considered to correspond to the variability within the related school size class (Tab. 2). The number of tunas found in 1 aggregation zone, the largest considered school size, could thereby consist of 626.4 ± 305.5 individuals. To account for the variability of a particular school size class, the total number of fish per school (size class) was not assigned to a fixed value, but was selected randomly (with replacement, n = 1000) from the corresponding size class distribution.

Annual tuna densities in the GoL

From survey estimates, the annual mean densities $\bar{D}$, of both tuna schools (school densities) and absolute tuna numbers (tuna densities), were approximated for the strip and line transect approaches by:

$$\bar{D} = \frac{1}{r} \sum_{i=1}^{r} \hat{D}_i, \tag{3}$$

where $\hat{D}_i$ gives the previously calculated tuna school/total tuna number density of survey i of r total replicates (number of surveys) in the year concerned. The associated variance $V(D)$ of yearly densities was defined as follows

$$V(D) = \frac{1}{r(r-1)} \sum_{i=1}^{r} \left(\hat{D}_i - \bar{D} \right)^2. \tag{4}$$

Spatial distribution of tuna schools

As population size fluctuates, the habitat used by a species can also fluctuate (MacCall's theoretical basin model; MacCall 1990). We thus examined the spatial distribution of sighted tuna schools in the GoL to investigate whether the area used in the GoL has changed through time. Spatial densities were calculated from the number of sightings per year, weighted by the survey effort and the average of their respective size class (Tab. 2). To interpolate across sighted schools in the GoL, an axis-aligned bivariate normal kernel, given by the "kde2d" function from the R-package "MASS", was applied (Venables and Ripley 2002), using a bandwidth of 0.5 and on a square grid of 500 x 500 points (horizontal resolution: 6.7 km). To facilitate comparison between years, annual density distributions were weighted by the respective annual density estimates obtained from the line transect approach at truncation level of 4.5 km (5%).

RESULTS

We found a very consistent pattern between modeling approaches and density estimates in which the abundance index of juvenile ABFT derived from aerial surveys in the Gulf of Lions is 3 to 4 times higher over the recent period (2009--2012) than during the early 2000s (Figs. 5 & 6). Using this dataset, the abundance estimates derived from the line transect theory was more stable and robust to the different hypotheses about the truncation distances (Figs. 5 & 6). This substantial increase in the abundance index is concurrent with a substantial increase in the spatial extent where ABFT juvenile have been observed in the Gulf of Lions (Fig. 7).

Changes in school size

Different school sizes were consistently sighted during each survey year (Fig. 8). The number of observed tuna schools of all size classes significantly increased since 2003. The sighting frequency per school size commonly decreased with increasing school size. Aggregation zones were not observed before 2009 and were most frequent in 2010. In the same year, small schools were much less frequent than in other survey years between 2009 and 2012. In the early survey years, remarkably high numbers of large schools were found in 2003.

Detectability and line transect modeling

Best model fits for each truncation level, selected using AIC, were obtained from the multiple-covariate approach based on a hazard rate key-function (Fig. S2). Goodness of fit tests (Cramer-von Mises and Kolmogorov-Smirnov tests) performed well for all selected models (p > 0.05), with no significant deviation visible in the q-q plots. Models with the hazard rate key-function generally performed better than those of the half-normal, as they could better reproduce the spiked SDFD. Best fits across all truncation levels indicated significant effects on the detectability by the observer team, school size and the sea state (Beaufort scale). The observer team effect is considered as an interaction of observer and type of aircraft and is further described in Tab. S1. Sea state and school size had opposing effects on detectability, as expected. Larger swell and whitecaps caused a stronger decline in detectability with distance, while schools were easier to spot as their size increased.

School and tuna densities in the GoL

Estimated school densities indicated a very consistent and substantial increase in abundance irrespective of the modeling approach (strip or line transect; Fig. 5). Estimates up until 2003 were generally 3 to 4 times lower than those from 2009 onwards. However, line transect estimates were approximately twice as high as that of strip transects and appeared to be more stable across the different truncation levels applied. By contrast, school densities obtained by the strip transect approach commonly decreased with

250 lower truncation. Accordingly, their range accounted 0.0026−0.017 and 0.0018−0.014 schools km^{-2} at a
251 truncation level of 1.852 and 2.8 km (22% and 12.8% data truncation), respectively.
252 Tuna densities showed a similar increase from the early 2000s to the period 2009--2012, but were less
253 stable in the latter period. Similarly, strip transect results were significantly lower than those obtained
254 from the line transect approach. Both approaches indicated a high tuna density for 2010, coinciding with
255 the highest number of observed aggregation zones during the entire survey years (Fig. 5).

Spatial distribution of tuna schools

257 Spatial kernel densities of juvenile ABFT showed a marked increase during recent survey years as opposed
258 to those from 2000 to 2003 (Fig. 7). Considering all years, tuna densities were generally highest on the
259 continental slope and here during most of the survey years in the central or western region. Accordingly,
260 a clear center could be observed in 2009 and 2010. In contrast to the early survey years when the
261 distribution of tunas was largely restricted to the slope area, since 2009 the distribution of tunas was
262 much larger and tunas were frequently observed on the shelf area. This is also apparent from the frequency
263 at which tuna schools were sighted, at different depth contours, when weighted by the survey effort (Fig.
264 S3). Note that in 2010, flights and thus sightings were limited to the western region of the survey area
265 due to unsuitable weather conditions (Fig. S4).

DISCUSSION

267 In the present study, we used aerial surveys to estimate the abundance of juvenile ABFT in the North-
268 western Mediterranean Sea. Two statistical methods were applied to derive abundance estimates from
269 sighted tuna schools: strip and line transect approaches. The results obtained from both approaches
270 showed large similarities across the entire time series of both school and tuna densities. In particular, they
271 indicate a significant increase in juvenile ABFT abundance between the 2 time periods, i.e. 2000--2003
272 and 2009--2012. School and tuna densities remain high in the subsequent years that are also marked by
273 high intra-annual variability (i.e. high standard deviation in Figs. 5 & 6). Differences in school and tuna
274 densities are based on year-to-year variations in school size frequencies. In this regard, the occurrence of
275 aggregation zones during the most recent years likely reflects the observed increase in juvenile ABFT
276 abundance from 2003 to 2009. Apart from this observation, sighting frequencies of small schools increased
277 during the most recent years (2011--2012) in relation to medium and large schools, suggesting a decrease
278 in tuna densities while school densities remain stable. However, with regard to the higher variability of
279 2009--2010 tuna density estimates, it remains unclear whether this could indicate a trend.
280

Strip vs. line transect modeling

282 In general, estimates of the line transect approach were systematically higher and more stable across the
283 different truncation levels, indicating superior robustness. The lower estimates from the strip transect
284 approach suggest that some tuna schools were missed within the applied strip widths. This is also shown
285 by a rapid decrease in the frequency of school sightings with increasing distance. However, a further
286 reduction of the strip width would not only impair the spatial representativeness of the survey but also
287 result in the omission of a large number of sightings. The latter would artificially introduce surveys
288 with zero sightings, resulting in the distortion of annual averaged density estimates. These problems
289 demonstrate major constraints in the application of the basic strip transect theory to the presented
290 visual-based aerial surveys. An adaptive strip transect approach in which the strip width is not set to
291 a fixed value but is a function of the major factors influencing detectability (e.g. school size and sea
292 state; Fig. 1) may improve density estimates but would require further modeling efforts. This would
293 remove one of the main advantages of the strip transect approach, i.e. its simplicity. In this context,

294 the principle advantage of the line transect approach is its ability to incorporate detections over a large
295 sighting distance, thereby correcting for potential effects on detectability. This further explains the slight
296 differences in the trends of tuna density estimates between both approaches, as school size frequencies
297 are altered during the line transect modeling, considering school size as a covariate.
298

Effects of tuna behavior on abundance estimates

300 Differences in the temporal development of school and tuna densities are driven by the changes in the
301 school size distribution and concern mainly the weighting of the years 2010 and 2012, which were marked
302 by a high number of tuna aggregation zones and small schools, respectively. Accordingly, within the
303 2009−2012 period, school densities are lowest in 2010, while the corresponding tuna densities are of the
304 same level or even higher than those of surrounding years. By contrast, the opposite effect was found for
305 2012, high school densities (mainly from the line transect approach) but lower tuna densities. Generally,
306 tuna densities appear to be more reliable as they account for differences in school size. However, more
307 precise information on school size is needed to improve the accuracy of density estimates. In the current
308 method, school size is first classified during the surveys according to the observed size of the water
309 disturbance created by tunas, using a semiquantitative approach, and is then expressed in numbers of
310 fish, using information from PS catch data. This may not fully reflect the actual school size as the size
311 of the observed water disturbance likely depends on multiple factors besides tuna school size, e.g. the
312 temporal dynamics of the intensity of the feeding event or the vigor of the feeding activity (Fig. 1). In
313 addition, the estimated number of fish per school can contain large variations, especially for large schools,
314 as indicated by the evaluated PS dataset. Simultaneously conducted acoustic surveys could be used to
315 detect and estimate the biomass of pelagic fish below the water surface and its dependency on feeding
316 dynamics (Weber *et al.* 2013). In theory, such knowledge could also be gained by airborne LIDAR (Light
317 Detection And Ranging). However, light-weight and power-efficient LIDAR systems for tuna detection
318 that further allow real time processing are still under development (Schoen and Sibert 1996, Churnside
319 *et al.* 1998, Cowling *et al.* 2002).
320 Another compounding factor is that, unlike the case of marine mammals, surfacing is not an obligatory
321 behavior of tunas, although ABFT is an epipelagic species that preferentially occupies surface and
322 sub-surface waters (Fromentin and Powers 2005, Walli *et al.* 2009). A related problem concerns the
323 common occurrence of surveys with no sightings, which represent a major source of the variability in
324 annual abundance estimates. In fact, ABFT often disappear only to reemerge soon thereafter, usually
325 within a couple of days, indicating that they remained within or, close to, the survey zone. Therefore, it is
326 necessary to replicate the survey several times during the season to avoid any bias due to changes in tuna
327 behavior (Cowling *et al.* 2002, Bonhommeau *et al.* 2010). Such short-term changes in the distribution of
328 tunas are indeed likely caused by changes of environmental conditions. For example, strong continental
329 winds, known as Tramontane and Mistral, can cause the temperature of the surface layer in the GoL to
330 drop by up to 5°C within 1 day and produce local upwellings (Millot 1979). The wind-induced disturbance
331 of the epipelagic zone may affect the vertical distribution of zooplankton (Incze *et al.* 2001) and thus the
332 foraging behavior of small pelagic fish, the main prey of juvenile ABFT in the GoL. Accordingly, ABFT
333 may adapt their feeding mode and their vertical distribution (Fig. 1). Future studies should therefore
334 aim to assess the changes in the vertical and horizontal distribution patterns of ABFT in relation to
335 prevailing environmental conditions. Regional archival tagging data, as presented by Fromentin and
336 Lopuszanski (2013), can help to fulfill this task as shown in other studies (Cowling *et al.* 2002, Newlands
337 *et al.* 2006, Hobday *et al.* 2009). An important factor could represent changes in the mesoscale eddy and
338 frontal activity that are known to attract both tunas and their prey (Fiedler and Bernard 1987, Royer
339 *et al.* 2004, Schick *et al.* 2004). Mesoscale activity is high in the GoL, especially along the continental
340 slope (André *et al.* 2009), an area that also constitutes an important fishing ground for small pelagic fish
341 (Saraux *et al.* 2014). Tuna kernel densities presented here are highest in this region, while sightings of

tuna schools on the continental shelf are less common. These findings are in accordance with results of early research flights in 1989 and commercial tuna spotter data of 1996 and 1997 from the same region (Petit *et al.* 1990, Liorzou 2001).

Importance of aerial surveys for tuna management

The presented results demonstrate that aerial surveys, which are more commonly used to monitor marine mammal populations, are also suitable for ABFT in the Mediterranean. Marine mammals, such as striped dolphins, fin, and sperm whales, were also frequently observed during the surveys. Combined multi-species surveys could thus provide an opportunity for collaboration and reduce total survey effort and costs for both species groups. Additionally, larger areas could be covered. Aerial surveys of marine mammals and sea turtle abundance have already been conducted in other nursery areas of ABFT, such as in the Gulf of Genoa, the Adriatic and the Balearic Sea and provided crucial knowledge for the conservation of these endangered species (Carreras *et al.* 2004, Forcada *et al.* 2004, Fortuna *et al.* 2011, Lauriano *et al.* 2011, Panigada *et al.* 2011). While the presented time series is long enough to be used for stock assessment, an increase in its spatial representativeness would be needed to assess recruitment trends of eastern ABFT. This does not concern the GoL feeding ground as its spatial coverage is considered sufficient with aerial surveys being carried out from the coastline to high depth areas (>2000 m). However, additional aerial surveys on other key nursery areas of ABFT, as mentioned above, would greatly help improve the representativeness and hence the index of juvenile ABFT abundance based on aerial surveys (ICCAT 2011). This is of particular importance since changes in the index can also be related to changes in the distribution of schools due to environmental forcing or ecological changes, and thus be unrelated to management regulations.

The positive trend observed in juvenile ABFT abundance in the GoL is consistent with stock assessment outputs (ICCAT 2013). Moreover, large tuna school aggregation zones have been observed since 2009, which were not present in the previous years. These results likely reflect the success of the ABFT rebuilding plan that led, among other things, to a drastic decline of the catch in the surveyed area (Fromentin *et al.* 2014). To date, ABFT stock assessment relies primarily on fisheries-dependent information (i.e. CPUE) that have several limitations (ICCAT 2013, Fromentin *et al.* 2014). In particular, such information is strongly affected by changes in fishery strategy and management regulations. The implementation of the 2007 ABFT rebuilding plan had such effects (Fromentin *et al.* 2014). The increase in the minimum landing size together with a drastic reduction of the TAC and the fishing season have strongly impacted all the fisheries that formerly provided CPUE indices for ABFT assessment (ICCAT 2013). As such, while the ABFT rebuilding plan has very positive outcomes in terms of the stock size, it also impairs the ability of CPUE indices to track changes in ABFT abundance. The index of abundance presented here does not suffer these constraints and thus offers a critical opportunity to provide a fishery-independent survey that would facilitate the tracking of changes in ABFT abundance.

It is worth noting that the ICCAT has recently initiated an Atlantic-wide research program to develop fishery-independent abundance indices for ABFT to improve stock assessment (ICCAT 2011). In current pilot studies, aerial surveys on mature ABFT were conducted in several key Mediterranean breeding areas. Conservation of the southern bluefin tuna is even more advanced, as aerial surveys constitute one of the 2 key sources of information for the evaluation of the recently implemented management strategy for the southern bluefin tuna stock (Rich *et al.* 2012). Undoubtedly, aerial surveys are a promising tool to monitor large pelagic fish abundance and follow management measure efficiency, but their value critically relies on long-term coverage and thus necessitates a continuous and substantial effort that national or international programs can hardly guarantee. The implementation of a scientific quota, as suggested by Fromentin *et al.* (2014), could represent a way forward that would allow the development of long-term scientific surveys.

395 ## Supplementary material

396 Fig. S1: Surface feeding tuna schools of different school size, seen abeam the airplane (from up to down:
397 small, medium and large)
398 Fig. S2: Detection functions of best model fits averaged over estimated covariate levels (black line), with
399 illustrated scaled detection frequencies per perpendicular distance (grey).
400 Fig. S3: Binned violine plot showing the frequency of sighted tuna schools, at different depth contours,
401 weighted by the survey effort.
402 Fig. S4: Spatial kernel densities of survey effort per year.
403 Tab. S1: Summary of completed aerial surveys with number of detected tuna schools per size class and
404 total effort.
405

406 ## LITERATURE CITED

407 André G, Garreau P, Fraunie P. (2009) Mesoscale slope current variability in the Gulf of Lions. Interpreta-
408 tion of in-situ measurements using a three-dimensional model. Continental Shelf Research 29:407−423, doi:
409 10.1016/j.csr.2008.10.004

410 Andriolo A, Martins CCA, Engel MH, Pizzorno JL, Más-Rosa S, Freitas AC, Morete ME et al. (2006) The first
411 aerial survey to estimate abundance of humpback whales (***Megaptera movaeangliae***) in the breeding groung off
412 Brazil (Breeding Stock A). Journal of Cetacean Research and Management 8:307−311

413 Auder B, Lebret R, Iovleff S, Langrognet F. (2014) Rmixmod: An interface for MIXMOD. R package version 2.0.2.
414 `http://cran.r-project.org/package=Rmixmod`

415 Beavers SC, Ramsey FL. (1998) Detectability analysis in transect surveys. The Journal of Wildlife Management
416 62:948−957

417 Bonhommeau S, Farrugio H, Poisson F, Fromentin JM. (2010) Aerial surveys of bluefin tuna in the western
418 Mediterranean Sea: retrospective, prospective, perspectives. Collective Volume of Scientific Papers ICCAT
419 65:801−811

420 Buckland ST, Anderson DR, Burnham KP, Laake JL. (1993) Distance Sampling: Estimating abundance of biological
421 populations. Chapman and Hall, London. 446 pp.

422 Buckland ST, Anderson DR, Burnham KP, Laake JL, Borchers DL, Thomas L. (2001) Introduction to Distance
423 Sampling: Estimating abundance of biological populations. Oxford University Press, Oxford. 448 pp.

424 Carreras C, Cardona L, Aguilar A. (2004) Incidental catch of the loggerhead turtle ***Caretta caretta*** off the Balearic
425 Islands (western Mediterranean). Biological Conservation 117:321−329, doi: 10.1016/j.biocon.2003.12.010

426 Churnside J, Wilson JJ, Oliver CW. (1998) Evaluation of the capability of the experimental oceanographic fisheries
427 lidar (FLOE) for tuna detection in the eastern tropical Pacific. NOAA Technical Memorandum ERL ETL-287.
428 Environmental Technology Laboratory. Boulder, CO. 74 pp.

429 Cowling A, Hobday A, Gunn J. (2002) Development of a fishery independent index of abundance for juvenile
430 southern bluefin tuna and improved fishery independent estimates of southern bluefin tuna recruitment through
431 integration of environmental, archival tag and aerial survey data. CSIRO Marine Research, Final report - FRDC
432 Projects: 96/118 and 99/105. 193 pp.

433 de Oliveira Alves MD, Schwamborn R, Gomes Borges JC, Marmontel M, Fernandes Costa A, França Schettini CA,
434 de Araújo ME. (2013) Aerial survey of manatees, dolphins and sea turtles off northeastern Brazil: Correlations
435 with coastal features and human activities. Biological Conservation 161:91−100, doi: 10.1016/j.biocon.2013.02.015

Di Natale A. (2011) ICCAT GBYP Atlantic-wide bluefin tuna research programme 2010. GBYP **coordinator's** detailed activity report for 2009-2010. Collective Volume of Scientific Papers ICCAT 66:995–1009

Eveson P, Farley J, Bravington M. (2012) The aerial survey index of abundance: updated analysis methods and results for the 2011/12 fishing season. CCSBT-ESC/1208/16, 17th meeting of the Scientific Committee, Commission for the Conservation of Southern Bluefin Tuna, 27–31 August 2012, Tokyo, Japan. 25 pp.

Farrugio H, Duclerc J, Tournier H. (1977) La pêche du thon rouge au filet tournant le long des côtes françaises de Méditerranée. Science et Pêche 268:1–12

Fiedler PC, Bernard HJ. (1987) Tuna aggregation and feeding near fronts observed in satellite imagery. Continental Shelf Research 7:871–881, doi: http://dx.doi.org/10.1016/0278-4343(87)90003-3

Forcada J, Gazo M, Aguilar A, Gonzalvo J, Fernandez-Contreras M. (2004) Bottlenose dolphin abundance in the NW Mediterranean: addressing heterogeneity in distribution. Marine Ecology Progress Series 275:275–287

Fortuna C, Holcer D, Filidei Jr E, Donovan G, Tunesi L. (2011) First cetacean aerial survey in the Adriatic Sea: Summer 2010. Seventh meeting of the ACCOBAMS Scientific Committee. Monaco, 29-31 March 2011. Document SC7-Doc06. 16 pp.

Fromentin JM, Bonhommeau S, Arrizabalaga H, Kell LT. (2014) The spectre of uncertainty in management of exploited fish stocks: The illustrative case of Atlantic bluefin tuna. Marine Policy 47:8–14, doi: 10.1016/j.marpol.2014.01.018

Fromentin JM, Bonhommeau S, Brisset B. (2013) Update of the index of abundance of juvenile bluefin tuna in the western Mediterranean Sea until 2011. Collective Volume of Scientific Papers ICCAT 69:454–461

Fromentin JM, Lopuszanski D. (2013) Migration, residency, and homing of bluefin tuna in the western Mediterranean Sea. ICES Journal of Marine Science 71:510–518, doi: 10.1093/icesjms/fst157

Fromentin JM, Powers JE. (2005) Atlantic bluefin tuna: population dynamics, ecology, fisheries and management. Fish and Fisheries 6:281–306, doi: 10.1111/j.1467-2979.2005.00197.x

Fujioka K, Hobday AJ, Kawabe R, Miyashita K, Honda K, Itoh T, Takao Y. (2010) Interannual variation in summer habitat utilization by juvenile southern bluefin tuna (*Thunnus maccoyii*) in southern Western Australia. Fisheries Oceanography 19:183–195, doi: 10.1111/j.1365-2419.2010.00536.x

Hobday A, Kawabe R, Takao Y, Miyashita K, Itoh T. (2009) Correction factors derived from acoustic tag data for a juvenile southern bluefin tuna abundance index in southern Western Australia. *In* Tagging and Tracking of Marine Animals with Electronic Devices SE - 24, edited by Nielsen J, Arrizabalaga H, Fragoso N, Hobday A, Lutcavage M, Sibert J. Volume 9 of *Reviews: Methods and Technologies in Fish Biology and Fisheries*, Springer Netherlands. pp. 405–422

Hoggard W. (1995) Aerial survey applications for assessing bluefin tuna abundance, distribution, and age structure in the Northwest Atlantic: a pilot study. Collective Volume of Scientific Papers ICCAT 45:151–154

ICCAT. (2006) Recommendation by ICCAT to establish a multi-annual recovery plan for bluefin tuna in the Eastern Atlantic and Mediterranean. Recommendation 06-05. Madrid, Spain. 14 pp.

ICCAT. (2011) 2011 GBYP Workshops on aerial surveys, and operational meetings on biological sampling and on tagging of bluefin tuna. Madrid, Spain - February 14-18, 2011. Collective Volume of Scientific Papers ICCAT 68:1–65

ICCAT. (2013) Report of the 2012 Atlantic bluefin tuna stock assessment session. Collective Volume of Scientific Papers ICCAT 69:1–198

Incze LS, Hebert D, Wolff N, Oakey N, Dye D. (2001) Changes in copepod distributions associated with increased turbulence from wind stress. Marine Ecology Progress Series 213:229–240, doi: 10.3354/meps213229

Ingram Jr GW, Alemany F, Alvarez D, García A. (2013) Development of indices of larval bluefin tuna (*Thunnus thynnus*) in the western Mediterranean Sea. Collective Volume of Scientific Papers ICCAT 69:1057–1076

Josse E, Dagorn L, Bertrand A. (2000) Typology and behaviour of tuna aggregations around fish aggregating devices from acoustic surveys in French Polynesia. Aquatic Living Resources 13:183–192, doi: 10.1016/S0990-7440(00)00051-6

Laake J, Borchers D, Thomas L, Miller D, Bishop J. (2013) mrds: Mark-recapture distance sampling (mrds). R package version 2.0.5. `http://cran.r-project.org/package=mrds`

Lauriano G, Panigada S, Casale P, Pierantonio N, Donovan GP. (2011) Aerial survey abundance estimates of the loggerhead sea turtle *Caretta caretta* in the Pelagos sanctuary, northwestern Mediterranean Sea. Marine Ecology

487   Progress Series 437:291–302, doi: 10.3354/meps09261

488   Leroy B, Nicol S, Lewis A, Hampton J, Kolody D, Caillot S, Hoyle S. (2015) Lessons learned from implementing
489   three, large-scale tuna tagging programmes in the western and central Pacific Ocean. Fisheries Research
490   163:23–33, doi: 10.1016/j.fishres.2013.09.001

491   Liorzou B. (2001) Effect of spotter aircraft on CPUE indices and feasability study to obtain new abundance indices.
492   *In* BFTMED - Major improvements in our knowledge of eastern Atlantic bluefin tuna in the Mediterranean
493   (Fisheries, statistics and biology), final report of the EU Project 97/029. European Community – DG XIV,
494   Brussels, edited by Liorzou B. pp. 124–131

495   Lutcavage M, Kraus S. (1997) Aerial survey of giant bluefin tuna, *Thunnus thynnus*, in the Great Bahama Bank,
496   Straits of Florida, 1995. Fishery Bulletin 95:300–310

497   Lutcavage M, Newlands N. (1999) A strategic framework for fishery-independent aerial assessment of bluefin tuna.
498   Collective Volume of Scientific Papers ICCAT 49:400–402

499   MacCall AD. (1990) Dynamic geography of marine fish populations. Washington University Press, Seattle and
500   London. 153 pp.

501   Marques FFC, Buckland ST. (2004) Covariate models for the detection function. *In* Advanced Distance Sampling,
502   edited by Buckland S, Anderson DR, Burnham KP, Laake JL, Borchers DL, Thomas L. Oxford University Press,
503   Oxford, Oxford. Chapter 3, pp. 31–47

504   Marques TA, Andersen M, Christensen-Dalsgaard S, Belikov S, Boltunov A, Wiig O, Buckland ST et al. (2006)
505   The use of Global Positioning Systems to record distances in a helicopter line-transect survey. Wildlife Society
506   Bulletin 34:759–763, doi: 10.2193/0091-7648(2006)34[759:TUOGPS]2.0.CO;2

507   Millot C. (1979) Wind induced upwellings in the Gulf of Lions. Oceanologica Acta 2:261–274

508   Newlands NK, Lutcavage ME, Pitcher TJ. (2006) Atlantic bluefin tuna in the Gulf of Maine, I: Estimation of
509   seasonal abundance accounting for movement, school and school-aggregation behaviour. Environmental Biology
510   of Fishes 77:177–195, doi: 10.1007/s10641-006-9069-5

511   Panigada S, Lauriano G, Burt L, Pierantonio N, Donovan G. (2011) Monitoring winter and summer abundance
512   of cetaceans in the Pelagos sanctuary (Northwestern Mediterranean Sea) through aerial surveys. PLoS ONE
513   6:e22878, doi: 10.1371/journal.pone.0022878

514   Petit M, Stretta J, Farrugio H, Wadsworth A. (1990) HAREM (Halieutique et radar, Expérimentation en
515   Méditerranée). Potentialités du radar SAR en halieutique. Application à la pêche thonière de surface et à la
516   pêche artisanale. Collection Etudes et thèses. 122 pp.

517   Pierce BL, Lopez RR, Silvy NJ. (2012) Estimating animal abundance. *In* The Wildlife Techniques Manual Volume
518   2, edited by Silvy NJ, 7th Edition. Johns Hopkins University Press, Baltimore, MD. pp. 284–310

519   Polacheck T, Pikitch E, Lo N. (1998) Evaluation and recommendations for the use of aerial surveys in the assessment
520   of Atlantic bluefin tuna. Collective Volume of Scientific Papers ICCAT 48:61–78

521   R Core Team. (2014) R: A language and environment for statistical computing. `http://www.r-project.org/`

522   Rich H, Preece A, Davies C. (2012) Developing a management procedure based recovery plan for southern bluefin
523   tuna, Final report FRDC project 2011/034. CSIRO Marine and Atmospheric Research, Castray Esplanade,
524   Hobart, TAS, Australia. 153 pp.

525   Royer F, Fromentin JM, Gaspar P. (2004) Association between bluefin tuna schools and oceanic features in the
526   western Mediterranean. Marine Ecology Progress Series 269:249–263, doi: 10.3354/meps269249

527   Saraux C, Fromentin JM, Bigot JL, Bourdeix JH, Morfin M, Roos D, Van Beveren E et al. (2014) Spatial structure
528   and distribution of small pelagic fish in the Northwestern Mediterranean Sea. PloS ONE 9:e111211, doi:
529   10.1371/journal.pone.0111211

530   Schick RS, Goldstein J, Lutcavage ME. (2004) Bluefin tuna (*Thunnus thynnus*) distribution in relation to sea surface
531   temperature fronts in the Gulf of Maine (1994–96). Fisheries Oceanography 13:225–238, doi: 10.1111/j.1365-
532   2419.2004.00290.x

533   Schoen C, Sibert J. (1996) Feasibility of dual mode Lidar for pelagic fish surveys. SOEST 96-02, IIMAR Contribution
534   96601. 18 pp.

535   Scott JM, Flittner GA. (1972) Behavior of bluefin tuna schools in the eastern north Pacific Ocean as inferred from
536   fishermen's logbooks. Fishery Bulletin 70:915–927

537   Thomas L, Buckland ST, Burnham KP, Anderson DR, Laake JL, Borchers DL, Strindberg S. (2012) Distance

538 Sampling. *In* Encyclopedia of Environmetrics, edited by El-Shaarawi A, Piegorsch W, 2nd Edition. John Wiley
539 & Sons Ltd, Chichester, UK. pp. 687–697

540 Venables WN, Ripley BD. (2002) Modern Applied Statistics with S, 4th Edition. Statistics and Computing.
541 Springer, New York, NY. `http://books.google.fr/books?id=974c4vKurNkC`, doi: 10.1007/978-0-387-21706-2

542 Walli A, Teo SLH, Boustany A, Farwell CJ, Williams T, Dewar H, Prince E et al. (2009) Seasonal movements,
543 aggregations and diving behavior of Atlantic bluefin tuna (*Thunnus thynnus*) revealed with archival tags. PloS
544 ONE 4:e6151, doi: 10.1371/journal.pone.0006151

545 Weber TC, Lutcavage ME, Schroth-Miller ML. (2013) Near resonance acoustic scattering from organized schools of
546 juvenile Atlantic bluefin tuna (*Thunnus thynnus*). The Journal of the Acoustical Society of America 133:3802–12,
547 doi: 10.1121/1.4802646
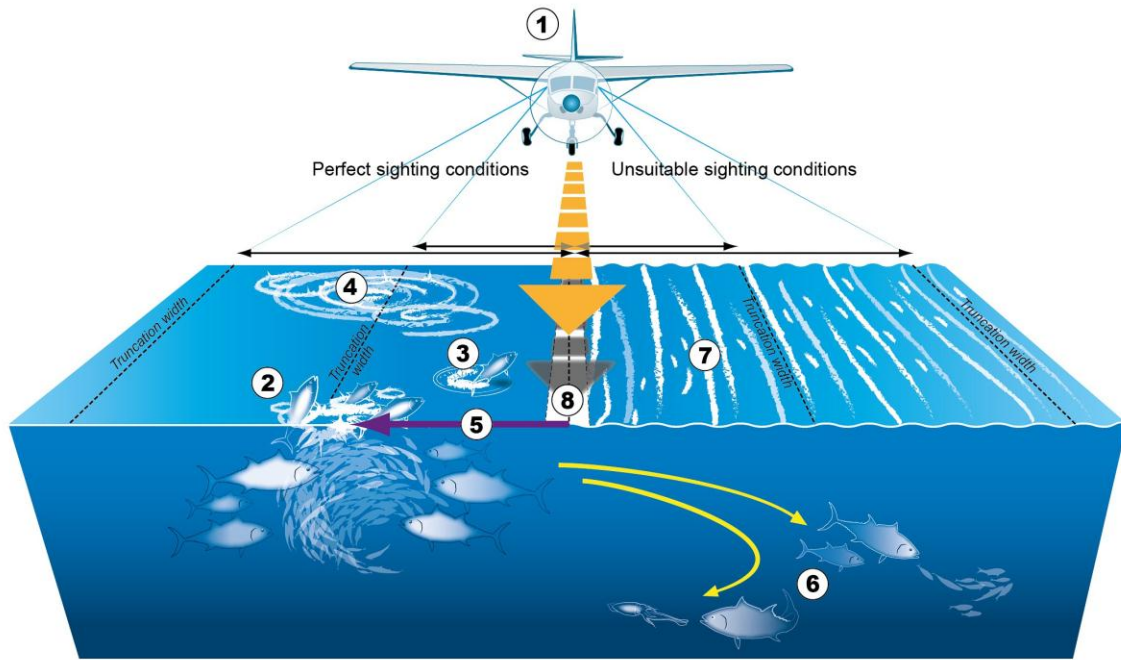
Fig. 1. Schematic drawing illustrating ABFT aerial surveys under perfect (left side) and impaired survey conditions (right side). (1) aircraft on transect line; (2) tuna school feeding with multiple jumpers; (3) small tuna school feeding with single tuna jumping; (4) large tuna school aggregation zones extending over several miles; (5) perpendicular distance; (6) tuna schools chasing in deeper waters; (7) waves with whitecaps; (8) blind spot for lateral detection
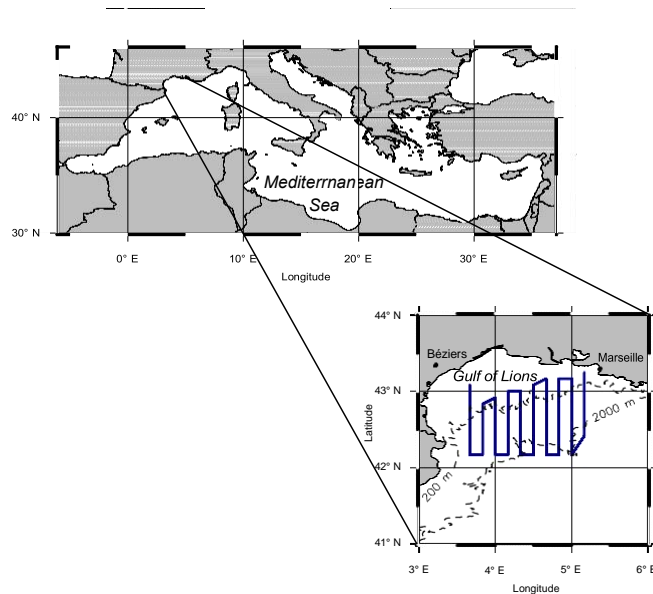
Fig. 2. Study area and transect lines of standard aerial surveys (blue). The dashed lines represent the 200 and 2000 m isobaths, indicating the continental shelf break of the Gulf of Lions.

Tab. 1. Overview of conducted tuna surveys per year and month. Effort measures represent the length of traveled transects.

Year	Effort (km)	Surveys with no sightings (% effort)	Surveys by month (% effort)		
			Aug	Sept	Oct
2000	3366	31.6	0	100	0.0
2001	4509	37.3	14	76	10.8
2002	5038	43.8	44	22	34.2
2003	6289	9.8	54	46	0.0
2009	4245	0.0	41	59	0.0
2010	2891	16.8	21	40	38.2
2011	5046	0.0	33	58	8.7
2012	4364	0.0	22	21	56.8
2000−2012	35749	16.9	31	51	17.4
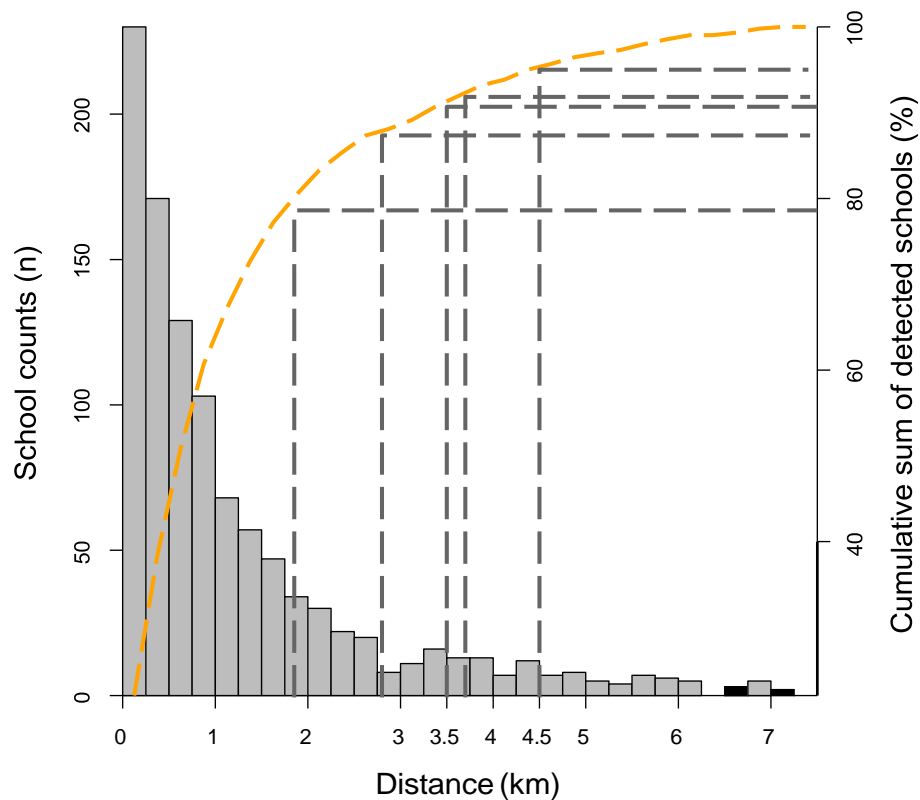
Fig. 3. Absolute frequencies and cumulated percentage (orange line) of the number of schools being detected per perpendicular distance to the transect route. Dotted and dash-dotted lines indicate the percentage of data included at the different truncation levels, used in the strip and line transect approaches, respectively.
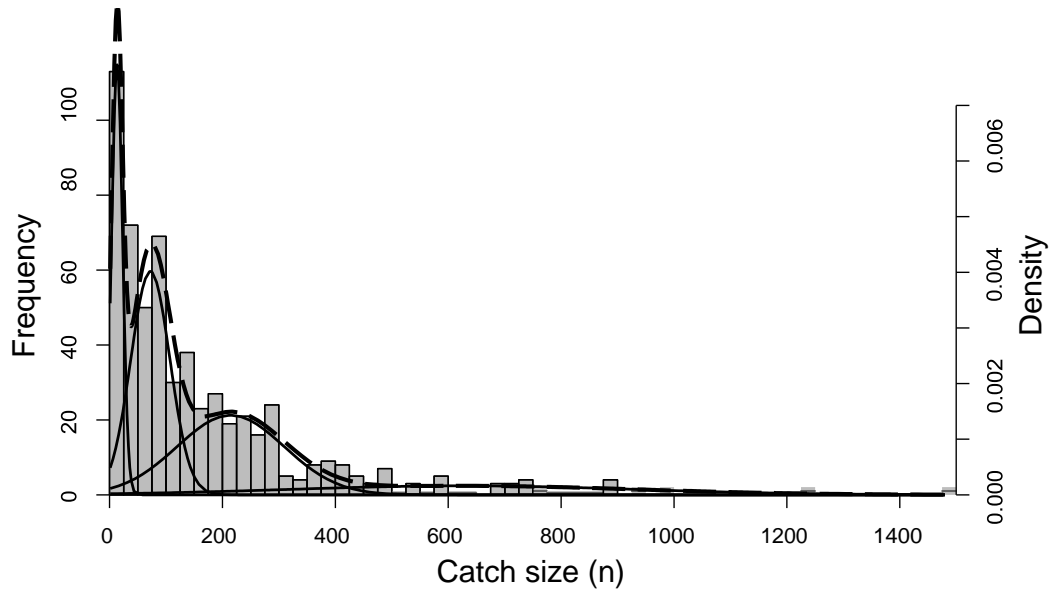
Fig. 4. Catch size of French purse seiners during August–October for 2000–2007, as well as fitted distributions of the Gaussian mixture model (solid lines) and their combined density (dashed line). The distributions are considered to correspond to size classes found during the aerial surveys.

Tab. 2. Average number of tuna per school size class ($\bar{x}$) and related standard deviation (σ) estimated by the Gaussian mixture (Fig. 4).

School size class	Mode	$\bar{x}$	σ
Small	1	13.3	9.6
Medium	2	72.3	34.7
Large	3	214.4	94.9
Aggregation	4	626.4	305.5
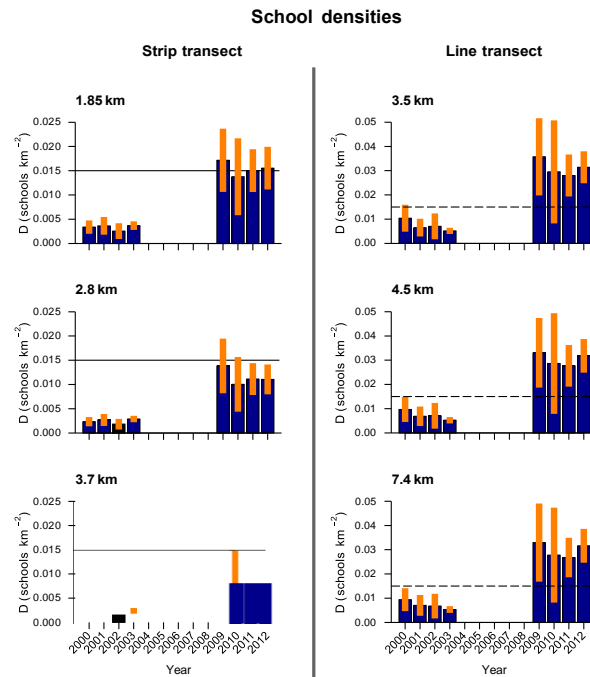
Fig. 5. School densities of tunas in the Gulf of Lions derived from the strip transect and line transect approach. Each row corresponds to the results of different truncation levels (1.85, 2.8 and 3.7 km for strip transects, 3.5, 4.5 km and untruncated data for line transects). The variance per yearly estimate is indicated by orange bars. The density of 0.015 schools km^{-2} is marked by the dashed reference line.
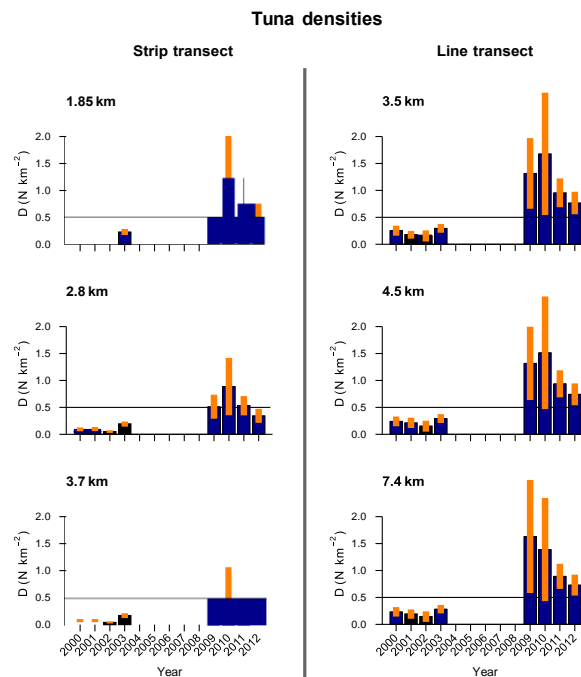
Fig. 6. Tuna densities in the Gulf of Lions derived from the strip transect and line transect approach. Each row corresponds to the results of different truncation levels (1.85, 2.8 and 3.7 km for strip transects, 3.5, 4.5 km and untruncated data for line transects). The variance per yearly estimate is indicated by orange bars. The density of 0.5 tunas km^{-2} is marked by the dashed reference line.
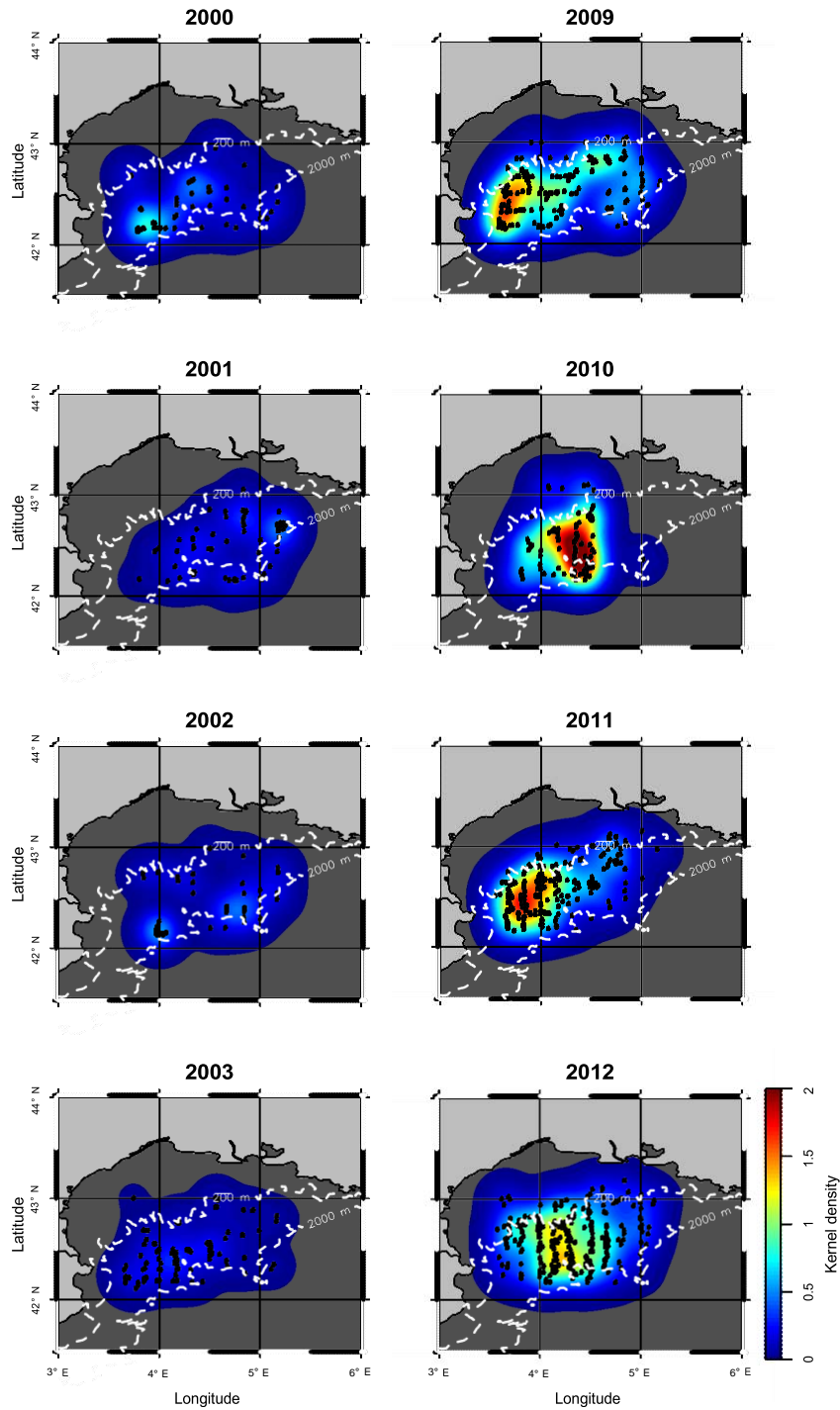
Fig. 7. Spatial kernel densities of total tuna counts in the Gulf of Lions per survey year weighted by the corresponding annual survey effort and tuna density estimates obtained from the line transect approach at truncation level of 4.5 km (5%). Sighting positions of tuna schools are illustrated by black dots. The white dashed lines give the 200 and 2000 m isobaths, indicating the continental shelf break of the Gulf of Lions.
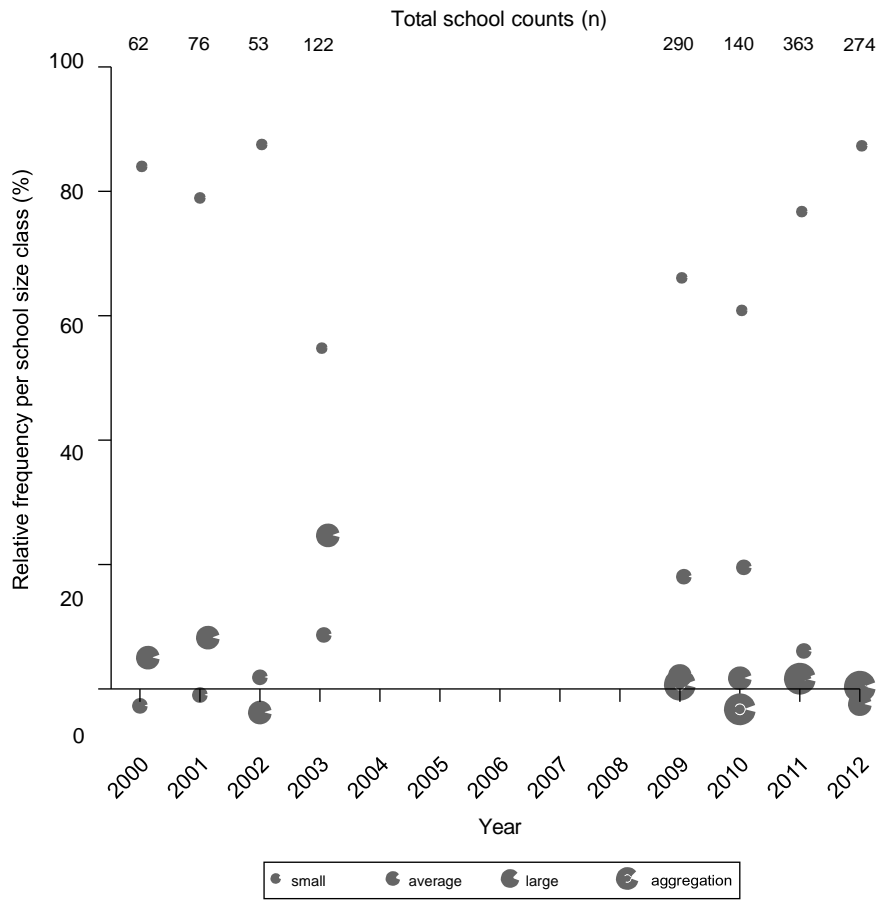
Fig. 8. Relative frequencies of different school size classes during each survey year.
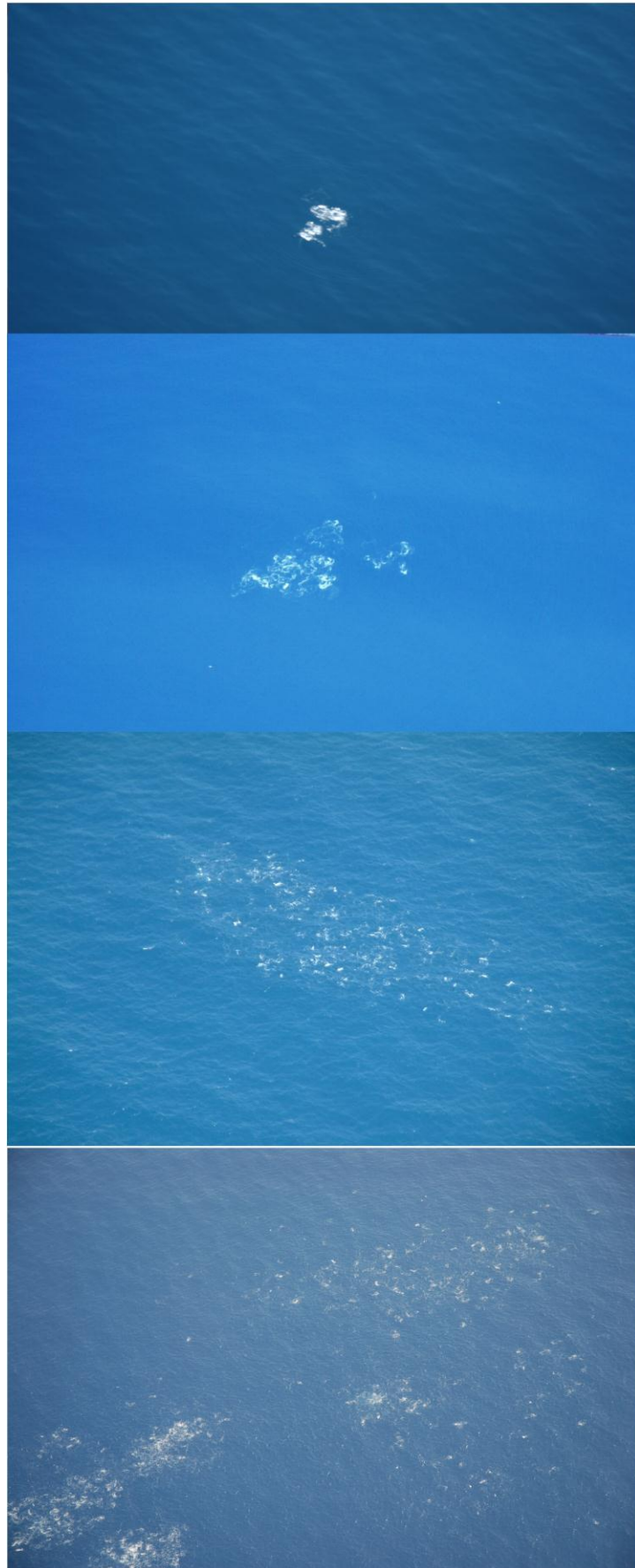
Fig. Sl. Surface feeding tuna schools of different school size, seen abeam the airplane (from up to clown: small, medium, large and subsection of an aggregation zone)
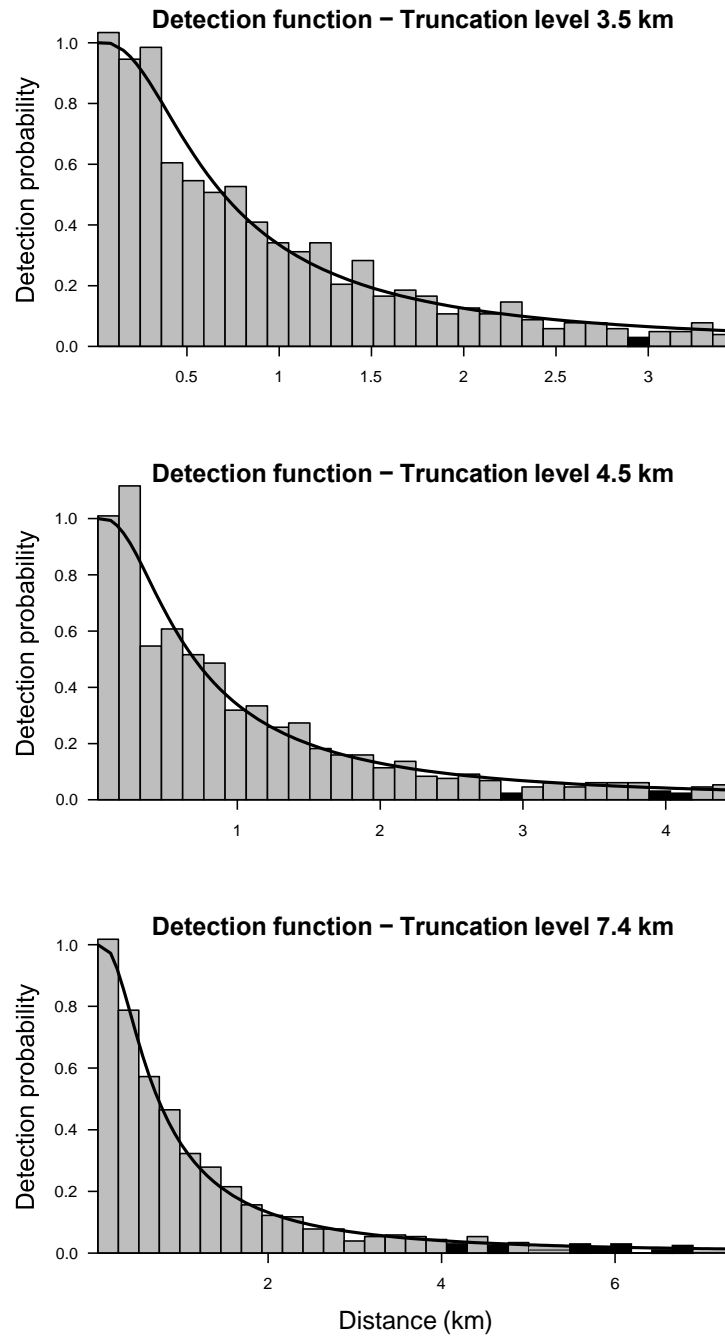
Detection function − Truncation level 3.5 km

Detection function − Truncation level 4.5 km

Detection function − Truncation level 7.4 km

Fig. S2. Detection functions of best model fits averaged over estimated covariate levels (black line), with illustrated scaled detection frequencies per perpendicular distance (grey). Best fits across all truncation levels indicated significant effects on the detectability by the covariates: observer team, school size and the sea state (Beaufort scale).

Tab. S1. Summary of completed aerial surveys with number of detected tuna schools per size class and total effort. Each letter in the **"observer team"**-key refers to a unique observer.

Year	Survey date	Observer Team	Number	pPane	Number of detections per school size Small	Medium	Large	Aggregation	Total	Effort (km)
2000	2000-09-06	ABC	3	Cessna C 337	8	4	2	0	14	619
2000	2000-09-08	ABC	3	Cessna C 337	0	0	0	0	0	485
2000	2000-09-09	ABC	3	Cessna C 337	23	3	4	0	30	619
2000	2000-09-13	ABC	3	Cessna C 337	11	0	0	0	11	485
2000	2000-09-23	ABC	3	Cessna C 337	0	0	3	0	3	580
2000	2000-09-24	AB	2	Cessna C 337	0	0	0	0	0	580
2001	2001-08-28	AB	2	Cessna C 337	8	1	2	0	11	619
2001	2001-09-12	AB	2	Cessna C 337	0	0	0	0	0	619
2001	2001-09-13	AC	2	Cessna C 337	24	3	0	0	27	485
2001	2001-09-20	ABC	3	Cessna C 337	0	0	0	0	0	580
2001	2001-09-21	AB	2	Cessna C 337	6	2	3	0	11	619
2001	2001-09-26	AC	2	Cessna C 337	1	0	0	0	1	619
2001	2001-09-27	AB	2	Cessna C 337	11	2	5	0	18	485
2001	2001-10-08	AB	2	Cessna C 337	0	0	0	0	0	485
2002	2002-08-05	AB	2	Cessna C 337	1	0	0	0	1	485
2002	2002-08-14	AB	2	Cessna C 337	16	0	1	0	17	619
2002	2002-08-21	AB	2	Cessna C 337	3	2	0	0	5	623
2002	2002-08-22	AB	2	Cessna C 337	0	0	0	0	0	485
2002	2002-09-12	AB	2	Cessna C 337	2	0	1	0	3	619
2002	2002-09-16	AC	2	Cessna C 337	19	7	0	0	26	485
2002	2002-10-08	AB	2	Cessna C 337	0	0	0	0	0	485
2002	2002-10-14	AB	2	Cessna C 337	0	0	0	0	0	619
2002	2002-10-24	AB	2	Cessna C 337	0	0	0	0	0	619
2003	2003-08-05	AB	2	Cessna C 337	17	6	6	0	29	619
2003	2003-08-07	AB	2	Cessna C 337	6	3	0	0	9	485
2003	2003-08-15	AB	2	Cessna C 337	0	0	0	0	0	619
2003	2003-08-18	AB	2	Cessna C 337	6	5	0	0	11	450
2003	2003-08-21	AB	2	Cessna C 337	1	3	2	0	6	619
2003	2003-08-27	AB	2	Cessna C 337	10	4	9	0	23	619
2003	2003-09-15	AB	2	Cessna C 337	0	0	3	0	3	619
2003	2003-09-18	AB	2	Cessna C 337	6	6	3	0	15	397
2003	2003-09-25	AB	2	Cessna C 337	5	1	11	0	17	619
2003	2003-09-26	AB	2	Cessna C 337	4	0	1	0	5	623
2003	2003-09-29	AB	2	Cessna C 337	1	0	0	0	1	623
2009	2009-08-27	ABD	3	Cessna C 337	4	2	0	0	6	619
2009	2009-08-28	ABD	3	Cessna C 337	1	0	0	0	1	619
2009	2009-08-31	ABD	3	Cessna C 337	21	12	1	0	34	485
2009	2009-09-07	ABD	3	Cessna C 337	17	22	17	0	56	623
2009	2009-09-08	ABD	3	Cessna C 337	14	7	16	0	37	102
2009	2009-09-10	ABD	3	Cessna C 337	49	30	17	2	98	557
2009	2009-09-11	ABD	3	Cessna C 337	9	5	2	0	16	623
2009	2009-09-23	AD	2	Cessna C 337	3	0	0	0	3	619
2010	2010-08-18	AD	2	Cessna C 337	15	5	1	0	21	619
2010	2010-09-15	AD	2	Cessna C 337	5	4	5	2	16	157
2010	2010-09-16	AD	2	Cessna C 337	1	0	0	0	1	485
2010	2010-09-22	AD	2	Cessna C 337	62	27	52	4	145	527
2010	2010-10-01	AD	2	Cessna C 337	1	0	0	0	1	619
2010	2010-10-06	AD	2	Cessna C 337	0	0	0	0	0	485
2011	2011-08-22	ADE	3	Cessna C 337	16	2	1	0	19	619
2011	2011-08-24	ADE	3	Cessna C 337	1	0	0	0	1	485
2011	2011-08-29	ADE	3	Cessna C 337	3	2	2	0	7	580
2011	2011-09-09	AD	2	Cessna C 337	15	17	4	0	36	619
2011	2011-09-15	ADE	3	Cessna C 337	18	4	7	0	29	623
2011	2011-09-21	ADE	3	Cessna C 337	45	23	16	0	84	619
2011	2011-09-26	AD	2	Cessna C 337	13	7	0	0	20	485
2011	2011-09-30	AD	2	Cessna C 337	27	7	13	4	51	580
2011	2011-10-03	AD	2	Cessna C 337	35	12	8	2	57	438
2012	2012-08-27	ZDE	3	Cessna 208 ISR	52	0	1	0	53	972
2012	2012-09-28	ZDE	3	Cessna 208 ISR	7	1	0	0	8	912
2012	2012-10-03	ZEF	3	Cessna 208 ISR	66	8	9	0	83	888
2012	2012-10-08	ZCF	3	Cessna 208 ISR	34	6	2	0	42	779
2012	2012-10-24	ZEF	3	Cessna 208 ISR	72	9	4	1	86	815
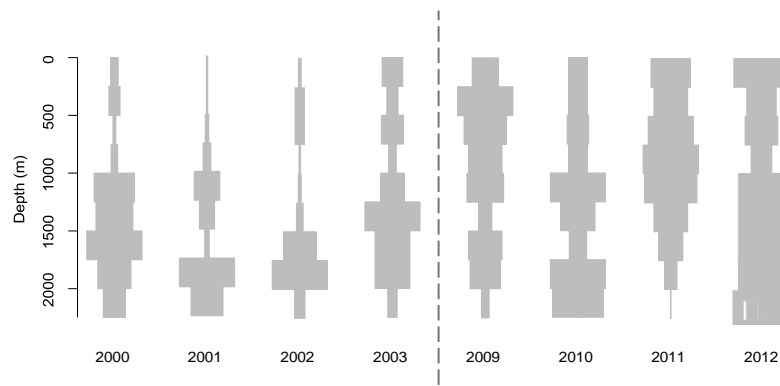
Fig. S3. Binned violine plot showing the frequency of sighted tuna schools, at different depth contours, weighted by the survey effort.

Fig. S4. Kernel densities of survey effort per year.